

# Study on Hypotheses for Simple Numerical Evaluation of Soil-Embedded Structure Interaction

by

Kazuo KONAGAI<sup>1</sup> and Mitsuhiro MAEHARA<sup>2</sup>

## 1. Introduction

In order to study soil-structure interaction, wave dissipation from a structure into the surrounding ground with an infinite spread must be taken into account. Numerical analyses employing the elastic wave theory are rational approaches in which the effect of wave dissipation is taken into account. Some assumptions have been adopted to make the analyses simple. Those include that the vertical ground motion is negligibly small in comparison with the horizontal (lateral) one. Many researchers<sup>(1),(2)</sup> made use of this assumption when they studied the dynamic response of a structure embedded in an elastic stratum. Their work yielded a lot of important findings. However, it should be noted that the dynamic response of an embedded structure differs in essence from that of the surrounding soil. This difference leads to fairly strong vertical ground motion in the vicinity of the structure. It goes without saying that the ground surface is free of normal and shear stresses. Thus, the incorporation of the stress-free surface condition into the analysis becomes very important when the surface motion of the surrounding soil has a pronounced effect on the motion of the embedded structure.

This paper discusses some of the customarily used assumptions in simple soil-embedded structure interaction analyses. The arguments for this discussion are based on some achieved numerical and experimental results.

## 2. Simple Numerical Approach for Interaction Analyses

Tamura and Suzuki<sup>(3)</sup> developed the quasi-three-dimensional ground model for earthquake response evaluation of a soft soil deposit on undulating bedrock. According to their method, first the surface layer is divided into finite number of vertical soil columns. Each column is "replaced" by a lumped mass-spring system, taking into account its fundamental vibration mode. These oscillators are then joined in a net of finite elements which represents the column-column interaction. After introducing a wave-transmitting boundary, Tamura and Konagai<sup>(4),(5)</sup> extended the application of the original method to the evaluation of embedded structure's dynamic stiffness. This new approach made possible the incorporation of both wave dissipation and effects of

---

<sup>1</sup> Associate Professor, Institute of Industrial Science, University of Tokyo

<sup>2</sup> Graduate student, ditto.

undulating bed rock into the dynamic response analyses of an embedded structure.

After reducing the element's (lumped mass) size, their model converges a continuous plate supported on Winkler's spring. By assuming the surface layer as an infinite elastic medium with uniform thickness, the continuous plate is also supposed to be a homogeneous one. The governing equations for this plate are given in rectangular Cartesian coordinates as follows:

$$\frac{\partial^2 u}{\partial t^2} = v_p^{*2} \frac{\partial^2 u}{\partial x^2} + (v_p^{*2} - v_s^2) \frac{\partial^2 v}{\partial x \partial y} + v_s^2 \frac{\partial^2 u}{\partial y^2} - \omega_0^2 u - 2h\omega_0 \frac{\partial u}{\partial t} \dots (1)$$

$$\frac{\partial^2 v}{\partial t^2} = v_p^{*2} \frac{\partial^2 v}{\partial y^2} + (v_p^{*2} - v_s^2) \frac{\partial^2 u}{\partial x \partial y} + v_s^2 \frac{\partial^2 v}{\partial x^2} - \omega_0^2 v - 2h\omega_0 \frac{\partial v}{\partial t} \dots (2)$$

where,  $u, v$  = displacements in lateral  $x$  and  $y$  directions,  $t$  = time,  $v_p^*$  = longitudinal wave velocity,  $v_s$  = shear wave velocity,  $\omega_0$  = fundamental natural circular frequency of a soil column ( $=\sqrt{k/\rho}$ ),  $k$  = spring constant of Winkler model,  $\rho$  = density of plate,  $h$  = damping constant ( $=c/2\sqrt{k\rho}$ ) and  $c$  = coefficient of viscous damping of the Winkler model.

The assumptions of negligible vertical motion and stress-free surface are compatible with the plate theory, i.e. correspond to the solutions under plane-strain and plane-stress conditions, respectively. Longitudinal wave velocity  $v_p^*$  within the plate is expressed for different plane conditions as:

$$v_p^* = \sqrt{\frac{\lambda^* + 2\mu}{\rho}} \dots (3)$$

where,  $\lambda^* = \lambda$  (plane-strain condition) ....(4)

$\lambda^* = 2\lambda\mu/(\lambda+\mu)$  (plane-stress condition) ....(5)

$\lambda, \mu$  = Lamé's constants

The dynamic stiffness,  $S_H$ , of a rigid circular hole within this plate corresponds to the stiffness of the soil surrounding the embedded structure. Its rigorous solution is expressed in circular cylindrical coordinates as:

$$S_H = \pi \mu a_0^{*2} T \dots (6)$$

where

$$T = \frac{4K_1(b_0^*)K_1(a_0^*) + a_0^*K_1(b_0^*)K_0(a_0^*) + b_0^*K_1(a_0^*)K_0(b_0^*)}{b_0^*K_0(b_0^*)K_1(a_0^*) + a_0^*K_1(b_0^*)K_0(a_0^*) + a_0^*b_0^*K_0(a_0^*)K_0(b_0^*)} \dots (7)$$

$$a_0^* = \frac{i\omega r_0}{\mu} \sqrt{\rho - \frac{k}{\omega} + \frac{c}{i\omega}} \dots (8)$$

$$b_0^* = a_0^* \left( \frac{V_s}{V_p} \right) \dots (9)$$

$\omega$ =circular frequency and  $K_1, K_2$ =modified Bessel functions of the second kind.

Fig.1 shows the variation of  $S_H$  and the rigorous solution in frequency domain for a rocking massless rigid cylinder embedded in an infinitely spread soil stratum<sup>(1)</sup>. Since Tajimi's analysis neglects the vertical motion of soil stratum, the infinite plate supported on Winkler's model is assumed to be of plane-strain type. The very good agreement between these curves validates the adequacy of the present method. However, the different approach to obtain the dynamic stiffness through the plate theory, i.e. under either plane-strain or plane-stress condition sometimes

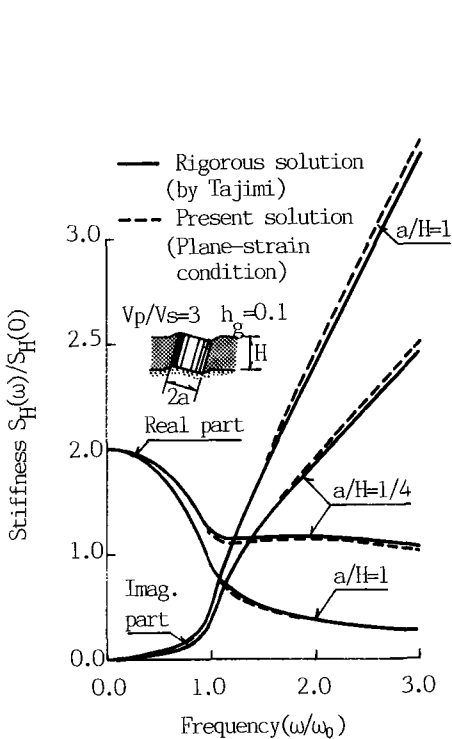


Fig.1 Variation of stiffness  $S_H$  with frequency

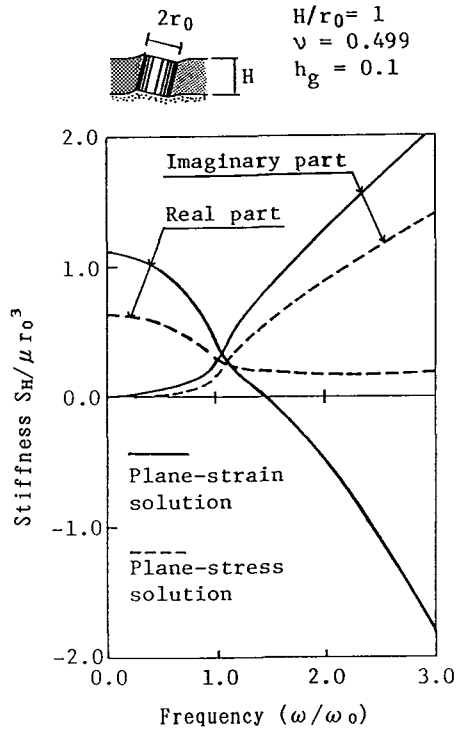


Fig.2 Variation of stiffness  $S_H/\mu r_0^3$  under different plate conditions

leads to a serious difference, as shown in Fig.2. This figure shows a comparison between the dynamic stiffness solutions for both plane-strain and plane-stress conditions. Poisson's ratio of the soil is 0.499. Under plane-strain condition, value of the static stiffness ( $\omega=0$ ) is relatively high. With increasing frequency,  $\omega$ , a steep descent of the real part of the stiffness solution occurs. This fact implies the increase of the soil mass which vibrates with the embedded cylinder. The difference between the two stiffness solutions urges us to study more precisely how the waves from an embedded structure propagate in the surrounding soil.

### 3. Wave Propagation from Embedded Cylinder

The real value of the longitudinal wave velocity,  $v_p$ , should lie between those values obtained for the plane-strain and plane-stress conditions. In order to observe the wave propagation, a model experiments were conducted. An artificial soil layer made of transparent poly-acrylamide gel is placed in an acrylic box. An acrylic hollow cylinder with radius of 50mm was embedded in it as shown in Fig.3. This cylinder has a small cone of brass on its bottom so that it can rock being supported on the bottom of the acrylic box. A force transducer with an aluminum plate was fixed on the cylinder wall at the level of 6cm above the artificial ground surface. A solenoid coil (0.18mH) was put close to the aluminum plate. The discharge of a capacitor (DC 3200V, 50 $\mu$ F) through the solenoid coil served as an impulsive energy source<sup>(6),(7),(8)</sup>.

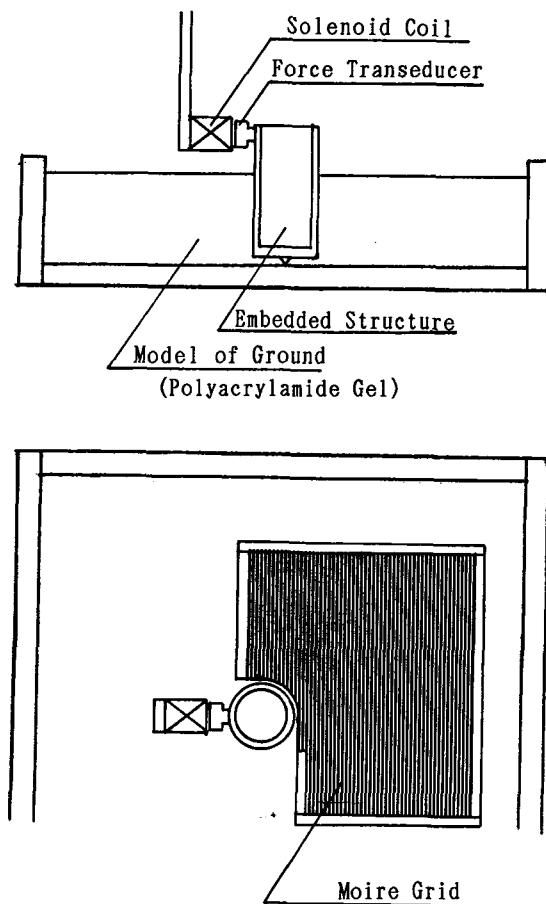
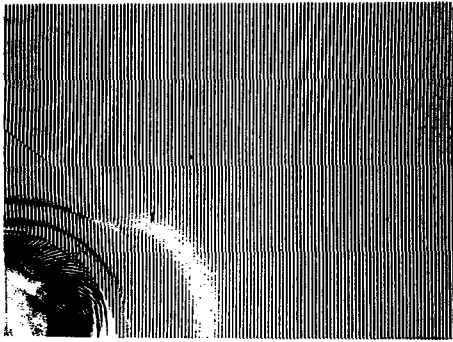
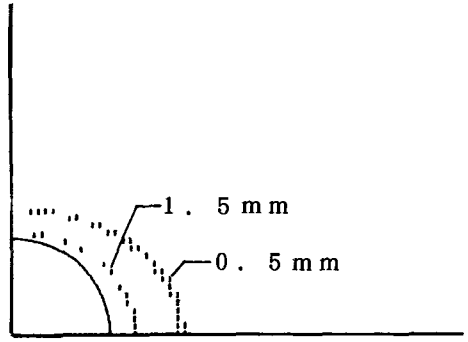


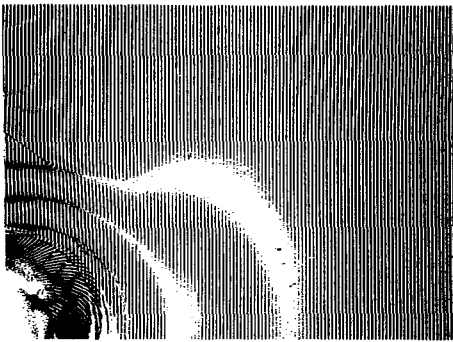
Fig.3 Model of stratum and embedded structure



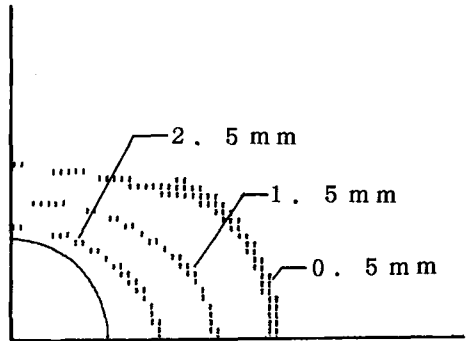
(a) 2.5 ms



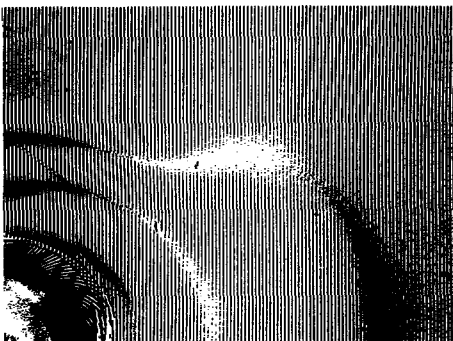
(a) 2.5 ms



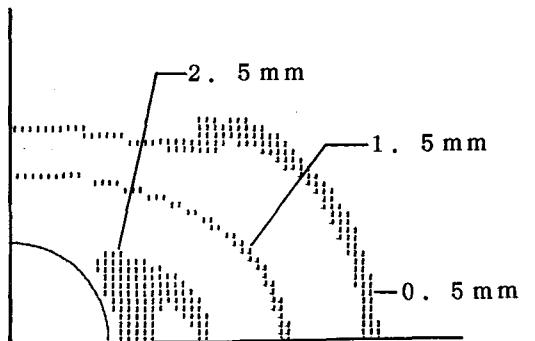
(b) 5.0 ms



(b) 5.0 ms



(c) 7.5 ms



(c) 7.5 ms

Photo.1 Observed moiré fringes

Fig.4 Simulated moiré fringes

Moire technique was used for visualizing the waves. A sheet of paraffin paper, on which black stripes of 0.5mm thickness were printed with special ink at an interval of 1.0mm, was put on the gel surface. Then the stripes were imprinted on it. The ingredients of this ink include synthetic rubber, phenol resin and pigment. Thus the stripes were very elastic and flexible, and capable to follow the motion of the gel very well. One of the customary approaches to record a transient phenomenon is to use a high-speed-framing camera. However, we adopted a simpler method by using an ordinary reflex camera, a xenon lamp and retarder to delay its lighting. This was possible because the aforementioned experimental apparatus can apply the same impulse force on the model repeatedly. Moire fringes can be visualized if pictures of the surface with the stripes, taken before and after excitation, are superimposed on one and the same film frame.

Photos. 1(a),(b),(c) show the observed moire patterns at every 2.5ms. Since an impulse was applied in the normal direction to the stripes, the moire fringe shows the contour of displacement in the direction of the impulse. A shear wave front propagates in the orthogonal direction to the excitation, and another clear wave front is seen in the longitudinal direction. The latter propagates with the double of the shear wave front speed. Since Poisson's ratio of the gel cured in water is about 0.5, Lamé's constant  $\lambda$  is much bigger than  $\mu$ , i.e. we can neglect  $\mu$  in equations (3) to (5). After substituting these constants in those equations,  $v_p^*$  for plate under plane-stress condition is obtained to be about the double of the shear wave velocity, while the value calculated under plane-strain condition is much bigger. Thus, so far as the longitudinal wave velocity on the surface is concerned, the plane-stress hypothesis predicts its value fairly well.

Figs.4 (a),(b) and (c) show simulated moire fringes by the finite difference method by using eqs.(1) and (2) in which  $v_p^*$  is assumed to be the double of the  $v_s$ . Observed displacement of the model structure was used as an input motion. Wave fronts fit well with the observed one. However, the displacement due to the longitudinal wave propagation is overestimated in this simulation.

## Conclusions

In order to study the wave dissipation from an embedded structure, which will affect much the soil-structure interaction, a model experiment for visualization of wave propagation was conducted. The artificial soil stratum was made of soft polyacrylamide gel. Moire grid with rubber-like flexibility was imprinted on the surface of the ground model. Moire fringes due to wave propagation caused by applied impulse force on an embedded cylinder (structure) were photographed. Conclusions of this study are summarized as follows:

(1) A shear wave front propagates in the orthogonal direction to the excitation, and another clear wave front is seen in the longitudinal direction. The latter propagates with the double of the shear wave front speed and is very slow in comparison with the longitudinal wave velocity of gel-like material cured in water.

(2) Propagation of both the shear wave and longitudinal wave fronts is well simulated by the finite difference method for the case of "plane-stress" plate being supported on Winkler's springs. The displacement due to propagation of the longitudinal wave is overestimated in this simulation.

### Acknowledgement

The authors acknowledge gratefully the financial support of the Ministry of Education, Science and Culture, Grant-in Aid for Scientific Research, No. 01302039. Special acknowledgement is made to Professor Choshiro Tamura, Department of Industrial Technology, Nihon University, for giving us important suggestions.

### APPENDIX I. REFERENCES

- (1) Tajimi, H.: Dynamic Analysis of a Structure Embedded in an Elastic Stratum, Proc., 4th World Conference on Earthquake Engineering, Vol.A-6, pp.54-69, 1969.
- (2) Novak, M. and Nogami, T.: Soil-Pile Interaction in Horizontal Vibration, Earthquake Engineering and Structural Dynamics, Vol.5, pp.263-281, 1977.
- (3) Tamura, C. and Suzuki, T.: A Quasi-Three-Dimensional Ground Model for Earthquake Response Analysis of Underground Structures - Construction of Ground Model -, "SEISAN KENKYU" (Monthly Jour., Inst., Industrial Science, Univ., Tokyo), Vol.39, No.1, pp.37-40, 1987.
- (4) Tamura, C. and Konagai, K.: Simple Approach for Evaluation of Dynamic Stiffness of Embedded Structure, Proc., 9th World Conference on Earthquake Engineering, Vol.III, pp.373-378, 1988.
- (5) Tamura, C., Konagai, K., and Suzuki, T.: Earthquake Response Analysis of Soft Soil Deposit on Undulating Bedrock, Report of the Institute of Industrial Science, University of Tokyo, Vol.36, No.5 (Serial No.234), pp.228-261, 1991.
- (6) Konagai, K., Takahashi, M. and Ogawa, S.: Experiments on Soil-Structure Interaction using Electromagnetic-Induction-Type Shock Wave Source, Proc., JSCE, Structural Eng./Earthquake Eng., Vol.2, No.1, pp.175-184, 1985.
- (7) Konagai, K., Koizumi, Y. and Ogawa, S.: Experiments on Soil-Pile Interaction Using Electromagnetic-Induction-Type Impulse Generator, Geotechnical Special Technical Publication on "Dynamic Behavior of Pile Foundations (Experiments Aspects)", ASCE, No.11, pp.91-101, 1987.
- (8) Konagai, K.: Simple Approach for Evaluation of Soil-Structure Interaction, "SEISAN-KENKYU" (Monthly Jour., of Inst., Industrial Science, Univ. of Tokyo), Vol.40, No.7, pp.1-8, 1988, (in Japanese).

## APPENDIX II. NOTATION

$c$  = viscous damping coefficient of the Winkler's model,  
 $h = c/2\sqrt{k\rho}$ , damping constant,  
 $k$  = spring constant of the Winkler's model,  
 $K_1, K_2$  = modified Bessel functions of the second kind.  
 $t$  = time,  
 $u$  = lateral displacement in  $x$  direction,  
 $v$  = lateral displacement in  $y$  direction,  
 $v_p^*$  = longitudinal wave velocity,  
 $v_s$  = shear wave velocity,  
 $\lambda$  = Lamé's constant,  
 $\mu$  = Lamé's constant,  
 $\rho$  = density of plate,  
 $\omega$  = circular frequency,  
 $\omega_0 = \sqrt{k/\rho}$ , fundamental natural circular frequency of a soil column,